Superconducting Integrated Receiver Based on Nb-AlN-NbN-Nb Circuits

Mikhail Yu. Torgashin, Valery P. Koshelets, Pavel N. Dmitriev, Andrey B. Ermakov, Lyudmila V. Filippenko, and Pavel A. Yagoubov

***Abstract*—The Superconducting Integrated Receiver (SIR) comprising in one chip a superconductor-insulator-superconductor (SIS) mixer and a phase-locked superconducting Flux Flow Oscillator (FFO) is under development for the international project TELIS. To overcome temperature constraints and extend operation frequency of the SIR we have developed and studied Nb-AlN-NbN-Nb circuits with a gap voltage Vg up to 3.7 mV and extremely low leakage currents ($\mathrm{Rj/Rn} > 30$). Based on these junctions integrated microcircuits comprising FFO and harmonic mixer have been designed, fabricated and tested; the radiation from such circuits has been measured at frequencies up to 700 GHz. Employment of NbN electrode does not result in the appearance of additional noise. For example, FFO linewidth as low as 1 MHz was measured at 600 GHz, that allows us to phase lock up to 92% of the emitted by FFO power and realize very low phase noise about −90 dBc. Preliminary results demonstrated uncorrected DSB noise temperature of the Nb-AlN-NbN SIR below 250 K at frequencies around 600 GHz.**

***Index Terms*—Josephson junctions, phase-locked oscillators, submillimeter wave integrated circuits, superconducting devices.**

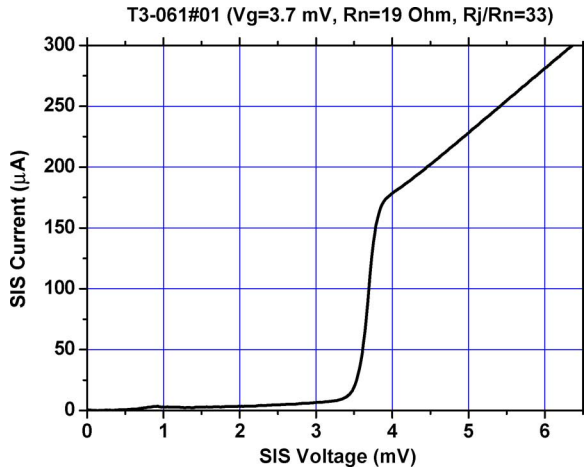

Fig. 1. IV characteristic of Nb-AlN-NbN junction ($\mathrm{S} = 2\ \mu\mathrm{m}^2$, $\mathrm{R_nS} = 37\ \Omega\ \mu\mathrm{m}^2$, $\mathrm{Jc} = 6.5\ \mathrm{kA/cm}^2$); Josephson supercurrent is suppressed by magnetic field.

I. Introduction

TELIS (TErahertz and submm LImb Sounder) [1] is a cooperation between European institutes to build a three-channel balloon-borne heterodyne spectrometer for atmospheric research. Many atmospheric trace gases have their rotational transitions in the sub millimeter and THz range, yielding a very rich spectrum. All three TELIS channels utilize superconducting SIS and HEB mixers for signal detection. The 550–650 GHz Superconducting Integrated Receiver (SIR) is developed by SRON Netherlands Institute for Space Research and Institute of Radio Engineering and Electronics (IREE). SIR comprises in one integrated circuit two superconductor-insulator-superconductor (SIS) mixers and a Flux-Flow Oscillator (FFO) as a Local Oscillator (LO). Up to now Nb-AlOx-Nb or Nb-AlN-Nb trilayers were successfully used for SIR fabrication. Traditional all-Nb circuits are being constantly optimized but there seems to be a limit for linewidth optimizations at certain boundary frequencies due to Josephson self-coupling (JSC) effect [2] as well as a high frequency limit, imposed by Nb gap frequency (∼700 GHz). That is the reason for novel types of junctions based on materials other than Nb to be developed.

II. Nb-AlN-NbN Tunnel Junctions

We reported earlier on the development of the high quality Nb-AlN-NbN junction production technology [3]. The implementation of an AlN tunnel barrier in combination with a NbN top superconducting electrode provides a significant improvement in SIS junction quality, see Fig. 1. The gap voltage of the junction $\mathrm{Vg} = 3.7\ \mathrm{mV}$. From this value and the voltage of the singularity corresponding to the difference of the superconducting gaps of the junction contacts $\mathrm{V}_\delta = (\Delta_{\mathrm{NbN}} - \Delta_{\mathrm{Nb}})/\mathrm{e} = 0.9\ \mathrm{mV}$ we can estimate the gap voltage of our NbN film as $\mathrm{Vg}^{\mathrm{NbN}} = 2.3\ \mathrm{mV}$.

The dependency of the ratio of subgap to normal state resistance (Rj/Rn) vs. critical current density (Jc) for different types of the Nb based junctions fabricated at IREE is presented in Fig. 2. One can see that the Nb-AlN-NbN junctions have very good quality at high current densities that is important for implementation in THz mixers. The same technique was further used to produce complicated integrated circuits comprising SIS and FFO in one chip.

III. Nb-AlN-NbN Flux Flow Oscillator

A Josephson Flux-Flow Oscillator [4]–[7] is known to be the most developed superconducting local oscillator for integra-

Manuscript received August 29, 2006. This work was supported in part by the RFBR projects 06-02-17206, ISTC project # 3174, NATO SfP Grant 981415, and inpart by the President Grant for Leading Scientific School 7812.2006.2.

M. Y. Torgashin, V. P. Koshelets, P. N. Dmitriev, A. B. Ermakov, and L. V. Filippenko are with the Institute of Radio Engineering and Electronics, Russian Academy of Science, Mokhovaya 11, 125009, Moscow, Russia, and also with the SRON Netherlands Institute for Space Research, 9700 AV Groningen, The Netherlands (e-mail: mikhail@hitech.cplire.ru).

P. A. Yagoubov is with the SRON Netherlands Institute for Space Research, 9700 AV Groningen, The Netherlands (e-mail: P.A.Yagoubov@sron.rug.nl).

Color versions of one or more of the figures in this paper are available online at http://ieeexplore.ieee.org.

Digital Object Identifier 10.1109/TASC.2007.898624

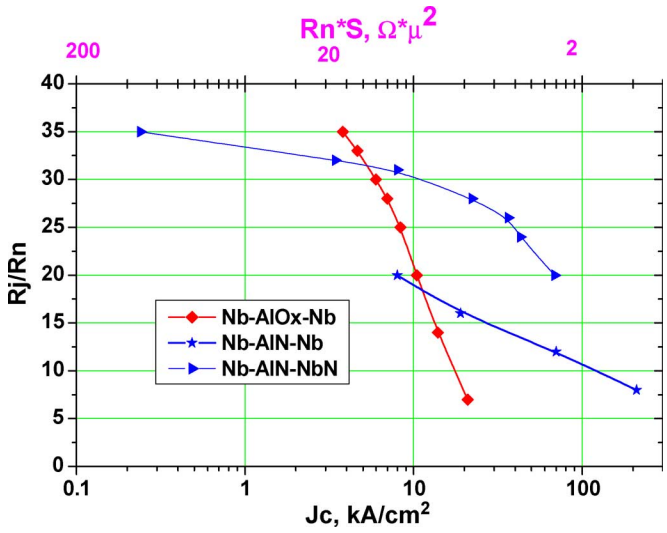

Fig. 2. The dependencies of Rj/Rn ratio vs. critical current density Jc for junctions fabricated at IREE.

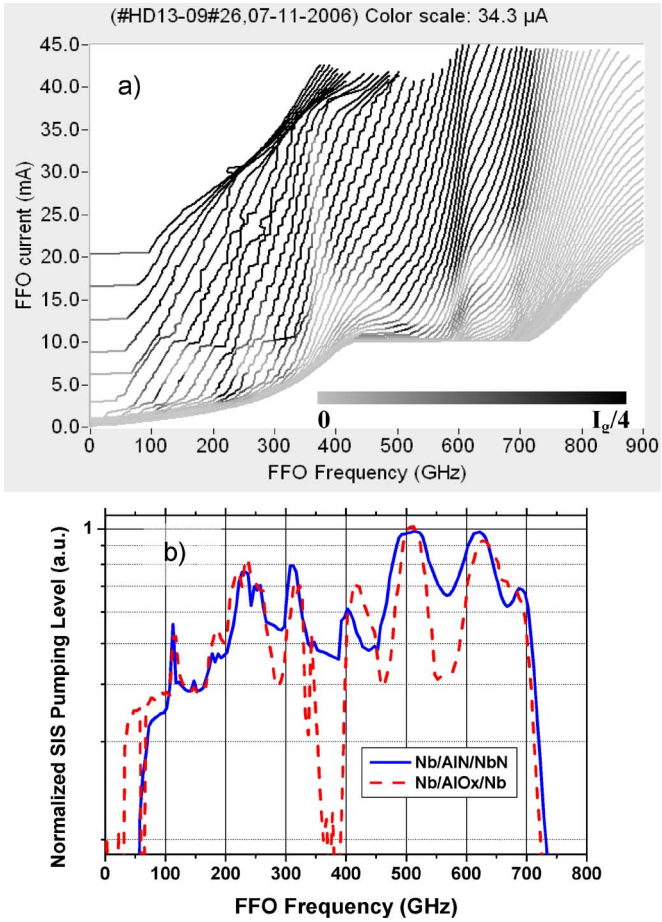

Fig. 3. (a) IVCs of the Nb-AlN-NbN-Nb FFO measured at different magnetic fields produced by the integrated control line. The voltage recalculated into frequencies according to Josephson relation. The tone scale shows the level of the DC current rise at the HM induced by the FFO. Black area marks the region of the FFO parameters where the induced by FFO HM current exceeds 25% of the Ig. This level is well above the optimal value for an SIS-mixer operation. (b) The maximum current detected by HM at $\mathrm{V} = 2.5$ mV normalized on the current rise at the HM gap voltage as a function of the FFO frequency (see Fig. 4). Dashed line—similar characteristic of Nb-AlOx-Nb FFO given for comparison. The target range for matching is 450–650 GHz. Good pumping level at low frequencies is due harmonics of Josephson radiation.

tion with SIS mixers [8]. The results of the development of the Nb-AlOx-Nb FFO, it's linewidth at different frequencies and ability to work in phase-locked mode were widely presented in publications (see [9] for example). Below we present the detailed results of the novel Nb-AlN-NbN junction investigation. The idea of using NbN or NbTiN is not new [10], but this materials are usually implemented in THz-range SIS mixers or for flux-flow oscillators aimed at frequencies above Nb gap frequency, up to 1.3 GHz [11] due to their high gap voltages and comparably high RF-losses. We used upper NbN both for the SIS mixers of micron and sub-micron sizes and for hundreds micron long FFOs. The idea was to investigate such type of junctions and determine their prospects for Superconducting Integrated Receiver at frequencies around 550–650 GHz (TELIS project).

Since the desired frequency range for the new devices lies below Nb gap frequency, the use of Nb matching structures is preferable due to lower losses of Nb compared to NbN. At the same time all of the lithography masks developed for the Nb SIR can be used directly for the fabrication of receivers with the Nb-AlN-NbN junctions because a small change of the FFO impedance due to AlN and NbN replacing AlOx and upper Nb doesn't cause strong impedance changes and mismatch. General behavior of the new devices is similar to the all-Nb chips; even the control currents, necessary to provide magnetic bias for FFO, were nearly the same for the similar design FFOs.

Fig. 3(a) present a family of current-voltage curves of an FFO, each measured at different magnetic field, provided by conducting current through a special control line (from 10 mA for the first curve (left), to 80 mA for the last curve in the right part of the graph). FFO here is a long Josephson junction with overlap geometry, the length of the junction is $\mathrm{L} = 400\ \mu\mathrm{m}$, its width $\mathrm{W} = 14\ \mu\mathrm{m}$, critical current density approximately $7\ \mathrm{kA/cm^2}$. The pumping current of the SIS junction induced by FFO is shown in Fig. 3(a) by gray scale; dependence of this current on FFO frequency is presented in Fig. 3(b). The profile, presented in this picture is determined by the maximum power, supplied from the FFO to harmonic SIS mixer and this in turn is determined by the quality of matching between the oscillator and mixer. As one can see the maxima of the envelopes for the Nb-AlOx-Nb samples and samples with Nb-AlN-NbN combined with upper Nb wiring coincide very well and the pumping curve for NbN is even smoother in the target region 500–700 GHz. Thus the masks developed for the standard all-Nb SIRs can be used for the Nb-AlN-NbN SIR fabrication without any modification.

In Fig. 4 typical current-voltage dependencies of a Nb-AlN-NbN SIS junction (area $\sim\ 2\ \mu\mathrm{m}^2$), pumped by a Nb-AlN-NbN FFO (solid line—unpumped IVC, dotted lines—pumped by the FFO at different frequencies). The frequency, calculated from the first photon-assisted tunneling step as $f_{LO} = e(Vg - Vstep)/h$, where $Vg = 3.67$ mV is the SIS gap voltage, e—electron charge, h—Plank's constant, is in agreement with the frequency calculated from the FFO bias voltage through Josephson relation $\mathrm{f} = 2\ \mathrm{eV/h}$. One can

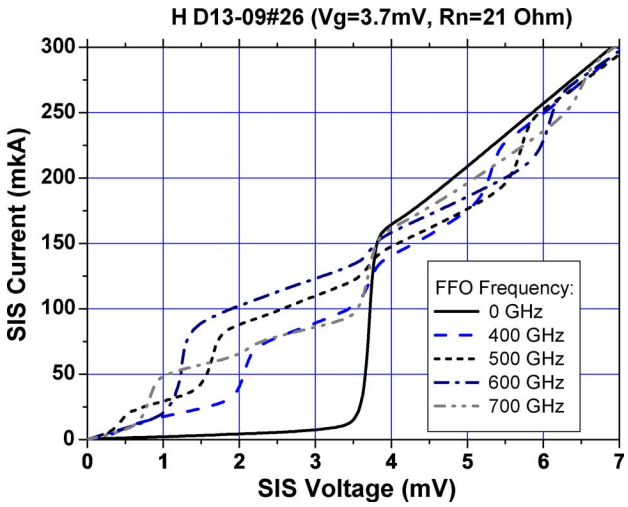

Fig. 4. The IVC of an SIS mixer. The unpumped—solid curve, pumped at different frequencies—dashed and dotted lines.

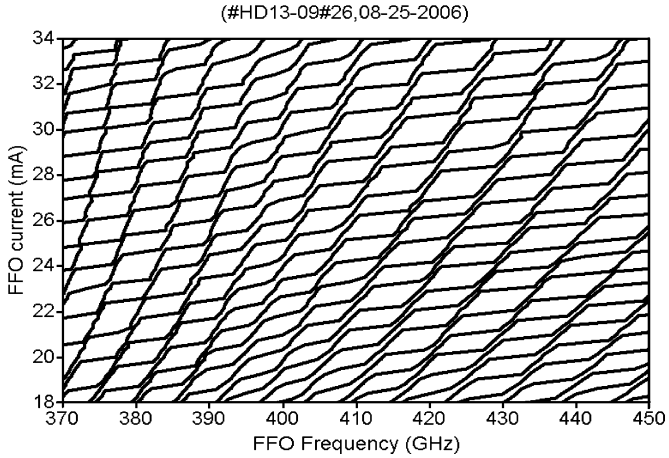

Fig. 5. A close-up of the Nb-AlN-NbN FFO IVC in Fiske steps region. One can see that the "vertical" parts of the steps link to form slanting lines. Along these lines continuous tuning is possible and the linewidth values are the lowest.

see that the FFO provides more than enough power for mixer pumping in the test circuits with low-loss matching circuits tuned between 500–700 GHz. For the SIR operation it's enough as well.

Although the Nb-AlN-NbN FFOs behave very similar to all-Nb ones there is a number of very important features that differ their properties from regular all-Nb FFOs (see Fig. 3(a)). First feature on the graph (around 500 GHz) is very likely due to singularity at $\Delta_{NbN} - \Delta_{Nb}$. The other feature at about 600 GHz where the curves get denser is a JSC boundary voltage [2]. Above this voltage internal damping of the FFO increases due to Josephson self-coupling effect. The JSC (absorption of the emitted by an FFO ac radiation by the quasi-particles in the cavity of the long junction) considerably modifies FFO properties at the voltages $\mathrm{V} \approx \mathrm{V_{JSC}} = 1/3 * \mathrm{Vg}$ ($\mathrm{V_{JSC}}$ corresponds to 600 GHz for the Nb-AlN-NbN FFO). Just above this voltage differential resistances increase considerably that results in FFO linewidth broadening if voltage is close above this point. This, in turn, makes difficult or impossible phase-locking of FFO in that region. For Nb-AlOx-Nb FFO a transition, corresponding *to* $V_{JSC} = Vg/3$ occurs around 450 GHz. So, we can cover the frequency gap from 450 to 550 GHz imposed by the gap value of all-Nb junctions using the Nb-AlN-NbN FFOs.

Continuous frequency tuning at frequencies below 600 GHz for the Nb-AlN-NbN FFOs of moderate length becomes possible though the damping is not high enough to completely suppress Fiske resonant structure at frequencies below Vg/3. For short junctions with small α—wave attenuation factor, the distance between the steps in this resonant regime can be as large, that it is only possible to tune the FFO at the certain set of frequencies. For 400 μm long Nb-AlN-NbN junction this is not the case—the quality factor of the resonator formed by a long Nb-AlN-NbN-Nb Josephson junction is not so high, the resonance steps are slanting and the distance between them is not so big (see Fig. 5). That allows us to set any voltage (and any frequency) below $\mathrm{V_{JSC}}$, but for each voltage only a certain set of currents should be adjusted. So, in this case we have the regions of forbidden bias current values, specific for each voltage below $\mathrm{V_{JSC}}$, instead of the forbidden voltage regions for Fiske regime in Nb-AlOx-Nb FFO. It is difficult to make automatic working point selection in this case, though not impossible.

IV. Linewidth of Nb-AlN-NbN-Nb FFO

We investigated the linewidth of Nb-AlN-NbN FFOs using the same setup and technique, as we used for all-Nb FFO linewidth measurement [12].The line shape is Lorentzian, same as for Nb-AlOx-Nb junctions. The expression for LW dependency on voltage and differential resistances [12], [13] is valid for Nb-AlN-NbN junctions as well, $\delta f = (2\pi/\Phi_0^2)\ (R_d^B + K * R_d^{CL})^2\ S_i(0)$; where $S_i(0)$ is the power density of low frequency current fluctuations, R_d^B and R_d^{CL} are differential resistances on bias and control line currents respectively. Note that K-factor is considerably different above and below $\mathrm{V_{JSC}}$.

Preliminary observations made for junctions of different topology let us assume that all the dependencies of LW on the geometrical parameters known for the all-Nb FFO hold for Nb-AlN-NbN. For example, we observe that the linewidth decreases with increasing junction width.

In Fig. 6 we present comparative graph of FFO linewidth. One can see that the linewidth of Nb-AlN-NbN-Nb FFO is twice as small up to 600 GHz. It should be mentioned that due to FS overlapping continuous tuning is possible and any desirable frequency could be realized. Several "stacked" stars at certain frequencies for the NbN FFO mean that the best linewidth value can be selected by adjusting FFO bias (all the linewidth values at the selected frequency are close and any will actually be good for measurements). Each star corresponds to an "allowed" bias current range at Fiske steps (as described above in Section II). Although FFO tuning is complicated on FS, the benefit in linewidth (and, consequently, spectral ratio) is worth the trouble—LW below 3 MHz can be achieved in the whole range between 350–600 GHz.

No additional noise sources were detected in the system with Nb-AlN-NbN samples, providing possibility to phase-lock an FFO in the whole operating range. In particular, the FFO linewidth as low as 1 MHz was measured at 600 GHz, that

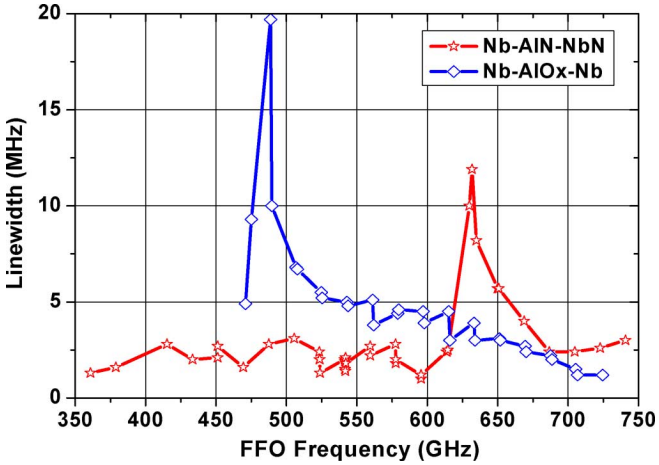

Fig. 6. The FFO linewidth dependency on frequency. Multiple stars on the red curve corresponding to a single frequency mean that the best point can be selected by the FFO working point adjustment in Fiske steps region.

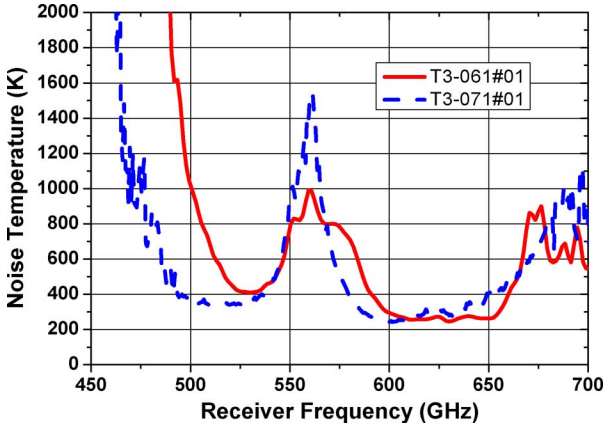

Fig. 7. The Nb-AlN-NbN-Nb SIR noise temperature dependency on LO frequency.

allows us to phase lock up to 92% of the FFO-emitted power and realize very low phase noise about −90 dBc.

V. Receiver Measurements

In TELIS flight cryostat the cooling of the Si lens with the SIR chip on it, magnetic shield, electronics and optics will be realized through the copper heat straps, connected to the cold plate of liquid helium container of the cryostat. Since for the safety reasons the pressure of vapors inside He vessel will be maintained above l atm., the temperature of the cold plate will be higher than 4.2 K and expected to be at the level of 4.5–5 K. This temperature rise added to overheating due to the thermal resistivity of all straps and thermal conductors between the chip and the cold plate significantly degrades the performance of Nb-AlOx-Nb junctions. We are sure that Nb-AlN-NbN FFOs can better cope with this amount of exceeding heat due to the higher gap voltage.

Several batches of the SIR chips of TELIS design with Nb-AlN-NbN-Nb junctions were produced and several chips were tested. They demonstrated good sensitivity in 500–700 GHz range (on Fourier-transform spectrometer, FTS) along with good DC characteristics. A very nice beam pattern has been observed with the sidelobes below −17 dB.

First noise measurements of non-optimized samples demonstrate that an uncorrected DSB noise temperature below 250 K can be achieved in the wide frequency region (Fig. 7). On the receiver noise temperature graph there is a sharp peak around 560 GHz—at least partly this peak is caused by very strong water absorption line at 557 GHz. It is necessary to carry out an evacuated hot-cold measurement to eliminate water vapor influence. We see that Nb-AlN-NbN junctions allow much improvement of receiver performance in 500 GHz region due to good FFO characteristics. In the upper frequency region around 700 GHz both all-Nb and Nb-AlN-NbN should have similar performance due to the limit imposed by Nb wiring at frequencies above the Nb gap frequency. Important that the Nb-AlN-NbN SIR noise temperature is very stable in respect to SIS mixer bias voltage, this dependence is almost flat from $V_{SIS} = 1.8$ to 3.3 mV.

The receiver frequency range can be adjusted by changing junction sizes, matching circuits and antenna parameters. In principle, it should be possible to create a receiver with best sensitivity in the chosen frequency range. The Nb-AlN-NbN junctions provide good opportunities both in the low and in high frequency regions.

References

[1] R. W. M. Hoogeveen *et al.*, "New cryogenic heterodyne techniques applied in TELIS: The balloon borne THz and submm limb sounder for atmospheric research," in *Proc. of SPIE, Infrared Spaceborne Remote Sensing XI*, 2004, vol. 5152, pp. 347–355.

[2] V. P. Koshelets, S. V. Shitov, A. V. Shchukin, L. V. Filippenko, J. Mygind, and A. V. Ustinov, "Self-pumping effects and radiation linewidth of Josephson flux flow oscillators," *Phys Rev B*, vol. 56, pp. 5572–5577, 1997.

[3] P. N. Dmitriev *et al.*, "High quality Nb-based integrated circuits for high frequency and digital applications," *IEEE Trans. Appl. Supercond.*, vol. 13, no. 2, pp. 107–110, 2003.

[4] T. Nagatsuma, K. Enpuku, F. Irie, and K. Yoshida, "Flux-flow type Josephson oscillator for millimeter and submillimeter wave region," *J. Appl. Phys.*, vol. 54, p. 3302, 1983.

[5] T. Nagatsuma, K. Enpuku, F. Irie, and K. Yoshida, *J. Appl. Phys.*, vol. 56, pt. II, p. 3284, 1984.

[6] T. Nagatsuma, K. Enpuku, F. Irie, and K. Yoshida, *J. Appl. Phys.*, vol. 58, pt. III, p. 441, 1985.

[7] T. Nagatsuma, K. Enpuku, F. Irie, and K. Yoshida, *J. Appl. Phys.*, vol. 63, pt. IV, p. 1130, 1988.

[8] V. P. Koshelets and S. V. Shitov, "Integrated superconducting receivers," *Superconductor Science and Technology*, vol. 13, pp. R53–R69, 2000.

[9] V. P. Koshelets *et al.*, "Superconducting integrated receiver for TELIS," *IEEE Trans. Appl. Supercond.*, vol. 15, pp. 960–963, 2005.

[10] Z. Wang, A. Kawakami, Y. Uzawa, and B. Komiyama, *J. Appl. Phys.*, vol. 79, no. 10, May 15, 1996.

[11] S. Kohjiro, Z. Wang, S. V. Shitov, S. Miki, A. Kawakami, and A. Shoji, "Radiation power of NbN-based flux-flow oscillators for THz-band integrated SIS receivers," *IEEE Trans. Appl. Supercond.*, vol. 13, no. 2, pp. 672–675, 2003.

[12] V. P. Koshelets *et al.*, "Phase locking of 270–440 GHz Josephson flux flow oscillator," *Rev. of Sci. Instr.*, vol. 71, no. 1, pp. 289–293, 2000.

[13] V. P. Koshelets *et al.*, "Optimization of the phase-locked flux-flow oscillator for the submm integrated receiver," *IEEE Trans. Appl. Supercond.*, vol. 15, pp. 964–967, 2005.